DOI: 10.15514/ISPRAS-2019-31(3)-18

Modeling Nonlinear Stabilization System on Clusters with Intel Xeon Phi Coprocessors

D.V. Melnichuk, ORCID: 0000-0002-6689-8904 <melnichukdv@sgu.ru>
Saratov State University,
83 Astrakhanskaya Street, Saratov, 410012, Russia

Abstract. Currently, cluster systems are widely used, the nodes of which use processors with a large number of cores. Effective software implementation on such computing systems requires that the corresponding mathematical models have a significant parallelism resource. For the problems of modeling of hybrid dynamical systems (HDS) a significant resource of parallelism is typical, since in this class of mathematical models the (theoretically infinite-dimensional) phase space of control objects with space-distributed parameters is isolated. The purpose of this work is to study the effectiveness of the software implementation on parallel computing systems of the class of modeling problems of the influence of typical nonlinearities and nonstationarity on the output vector function of the HDS. As an example, a nonlinear stabilization system for a mobile control object (the rocket taking into account the elastic deformations of its body) is considered.

Keywords: hybrid dynamical systems; processors with scalable architecture

For citation: Melnichuk D.V. Modeling of Angular Stabilization System on Processors with Scalable Architecture. Trudy ISP RAN/Proc. ISP RAS, vol. 31, issue 3, 2019. pp. 229-240. DOI: 10.15514/ISPRAS-2019-31(3)-18

Моделирование нелинейной системы стабилизации на кластерах с сопроцессорами Intel Xeon Phi

Д.В. Мельничук, ORCID: 0000-0002-6689-8904 <melnichukdv@sgu.ru>
Саратовский государственный университет имени Н.Г. Чернышевского,
410012, Россия, г. Саратов, ул. Астраханская, 83

Аннотация. В настоящее время широкое распространение получают кластерные системы, в узлах которых используются процессоры с большим числом ядер. Эффективная программная реализация на подобных вычислительных системах требует, чтобы соответствующие математические модели обладали значительным ресурсом параллелизма. Для задач моделирования комбинированных динамических систем (КДС) типичен значительный ресурс параллелизма, поскольку в данном классе математических моделей (теоретически бесконечномерное) фазовое пространство объектов управления с распределенными по пространству параметрами является изолированным. Целью работы является исследование эффективности программной реализации на параллельных вычислительных системах класса задач моделирования влияния типовых нелинейностей и нестационарности на выходные вектор-функции КДС. В качестве примера рассмотрена нелинейная система стабилизации подвижного объекта управления (ракеты с учетом упругих деформаций ее корпуса).

Ключевые слова: комбинированные динамические системы; процессоры с масштабируемыми архитектурами

Для цитирования: Мельничук Д.В. Моделирование системы угловой стабилизации на процессорах с масштабируемыми архитектурами. Труды ИСП РАН, том 31, вып. 3, 2019 г., стр. 229-240 (на английском языке). DOI: 10.15514/ISPRAS-2019-31(3)-18

1. *Introduction*

Currently, cluster systems are widely used, in the nodes of which one or several processors with a large number of cores are used. Examples include computing systems with new Intel Xeon processors with scalable architecture or computing systems with Intel Xeon Phi coprocessors that are used as virtual cluster nodes. Parallel computational architectures of this class are effective only when solving problems with a significant parallelism resource. In this case, classes of mathematical models that are effectively implemented on Intel Xeon Phi, will be effectively implemented on modern scalable Intel Xeon architectures.

Hybrid dynamical systems (HDS) [1, 2] are mathematical models of a number of technical systems containing control objects with lumped parameters and connected to them across the boundaries of control objects with distributed parameters (see fig. 1). HDS is characterized by input and output vector functions. The nonlinear system of angular stabilization of the movable control object with deformable body is the example [3, 4]. HDS are systems of ordinary differential equations (ODE) and partial differential equations (PDE) connected by means of boundary conditions (BC) and constraint's conditions (CC) under appropriate initial conditions (IC). For the problems of HDS modeling a significant resource of parallelism is typical, since the (theoretically infinite-dimensional) phase space of control objects with distributed parameters is isolated.

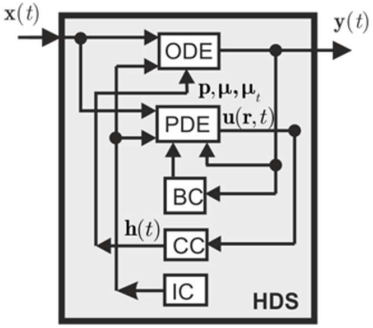

Fig. 1. HDS Structural scheme

2. *Related work*

MPI technology is standard for cluster systems with distributed memory, and both optimization of MPI itself [5] and parallel libraries [6] and algorithms based on it are relevant. Examples are problems of mathematical physics [7, 8], graph theory [9], sparse matrix factorization [10]. Optimization of parallel algorithms for cluster systems with many-core processors was considered in [11, 12]. If adaptive algorithms of numerical modeling are used or nodes of the cluster have different capacities, dynamic balancing of computational load is required [13]. For dynamic balancing of computational load on cluster systems, the MPI-MAP parallelization pattern was previously implemented [3]. The main theorems on the stability of linearized HDS are formulated and proved in [1, 2]. In work [4] adaptive algorithms of HDS parametric synthesis are offered. Modeling of systems of angular stabilization of movable control objects with deformable body was considered in [14, 3, 4].

3. *Problem formulation*

The purpose of this work is to study the effectiveness of the software implementation on parallel computing systems of the class of modeling problems of the influence of typical nonlinearities and nonstationarity on the output vector function of the HDS. We consider a similar [4] system of angular

stabilization of the movable control object (the rocket taking into account the deformations of its body), but providing stabilization both with respect to the vertical direction and with respect to the longitudinal axis, as well as a smooth change in the time of the thrust force of the rocket engine.

4. Parallel algorithms for modeling of hybrid dynamical systems

HDS with piecewise continuous input vector function $\mathbf{x}(t)$, $\mathbf{x}: \mathrm{R} \to \mathrm{R}^{N_x}$ and continuous output vector function $\mathbf{y}(t)$, $\mathbf{y}: \mathrm{R} \to \mathrm{R}^{N_y}$ correspond to equations

$$\dot{\mathbf{y}} = \mathbf{f}(\mathbf{x}, \mathbf{y}, \mathbf{h}, \mathbf{p}, \boldsymbol{\mu}, \boldsymbol{\mu}_t t); \dot{\mathbf{u}} = \mathbf{F}(\mathbf{u}, \mathbf{x}, \mathbf{y}, \dot{\mathbf{y}}, \boldsymbol{\mu}, \boldsymbol{\mu}_t t), \mathbf{r} \in \Omega$$
$$\mathbf{G}(\mathbf{u}, \mathbf{y}, \boldsymbol{\mu})|_S = 0, S = \partial\Omega; \mathbf{h} = \int_S \mathbf{H}(\mathbf{u}, \boldsymbol{\mu}) dS \qquad (1)$$
$$\mathbf{y}(0) = \mathbf{y}_0, \mathbf{u}(\mathbf{r}, 0) = \mathbf{u}_0(\mathbf{r})$$

Here $\mathbf{r} \in \mathrm{R}^{N_r}$ – are independent spatial coordinates of individual points of the object with distributed parameters, $\Omega \subset \mathrm{R}^{N_r}$ – area occupied by an object with distributed parameters, $\mathbf{f}: \mathrm{R}^{N_x} \times \mathrm{R}^{N_y} \times \mathrm{R}^{N_h} \times \mathrm{R}^{N_p} \times \mathrm{R}^{N_\mu} \times \mathrm{R}^{N_t} \to \mathrm{R}^{N_y}$, $\mathbf{h}: \mathrm{R} \to \mathrm{R}^{N_h}$, $\mathbf{u}(\mathbf{r}, t)$, $\mathbf{u}: \mathrm{R}^{N_r} \times \mathrm{R} \to \mathrm{R}^{N_u}$ – distributed output vector function, operators $\mathbf{F}: (\mathrm{R}^{N_r} \times \mathrm{R} \to \mathrm{R}^{N_u}) \times (\mathrm{R} \to \mathrm{R}^{N_x}) \times (\mathrm{R} \to \mathrm{R}^{N_y}) \times (\mathrm{R} \to \mathrm{R}^{N_y}) \times \mathrm{R}^{N_\mu} \times \mathrm{R}^{N_t} \to (\mathrm{R}^{N_r} \times \mathrm{R} \to \mathrm{R}^{N_u})$, $\mathbf{G}: (\mathrm{R}^{N_r} \times \mathrm{R} \to \mathrm{R}^{N_u}) \times (\mathrm{R} \to \mathrm{R}^{N_y}) \times \mathrm{R}^{N_\mu} \to (\mathrm{R}^{N_r} \times \mathrm{R} \to \mathrm{R}^{N_g})$, $\mathbf{H}: (\mathrm{R}^{N_r} \times \mathrm{R} \to \mathrm{R}^{N_u}) \times \mathrm{R}^{N_\mu} \to (\mathrm{R} \to \mathrm{R}^{N_h})$ correspond to partial differential equations, boundary conditions, and coupling conditions; $\mathbf{p} \in \mathrm{R}^{N_p}$ – feedback parameters; $\boldsymbol{\mu} \in \mathrm{R}^{N_\mu}$ – the parameters of model nonlinearities; $\boldsymbol{\mu}_t \in \mathrm{R}^{N_t}$ – parameters characterizing the unsteadiness of the system from the point of view of the automatic control theory; the point at the top indicates the time t differentiation. When $\boldsymbol{\mu} = \boldsymbol{\mu}_t = 0$ HDS (1) becomes linear stationary. After parametric synthesis, numerical simulation of the effect of typical nonlinearities and unsteadiness on the output vector function of a nonlinear HDS (1) is performed. In this case, the input vector function $\mathbf{x}(t)$ and the initial conditions $\mathbf{y}_0$, $\mathbf{u}_0(\mathbf{r})$ are fixed, and the components of the vectors $\boldsymbol{\mu}$ and $\boldsymbol{\mu}_t$ change with a fixed step within a parallelepiped. The element-by-element transformation of sequence $(\boldsymbol{\mu}_j, \boldsymbol{\mu}_{t_j})$, $j = 1,2,3,\ldots$ into a sequence of values characterizing the maximum and standard deviations of function $\mathbf{y}(t; \boldsymbol{\mu}_j, \boldsymbol{\mu}_{t_j})$ from $\mathbf{y}(t; 0,0)$ is parallelized

$$(\boldsymbol{\mu}_j, \boldsymbol{\mu}_{t_j}) \to (v_{1_j}, v_{2_j})^T, j = 1,2,3,\ldots; v_1 = \max_{0 \le t \le t_{\max}} |\mathbf{y}(t; \boldsymbol{\mu}, \boldsymbol{\mu}_t) - \mathbf{y}(t; 0,0)|$$
$$v_2 = \left[t_{\max}^{-1} \int_0^{t_{\max}} |\mathbf{y}(t; \boldsymbol{\mu}, \boldsymbol{\mu}_t) - \mathbf{y}(t; 0,0)|^2 dt\right]^{1/2}, t_{\max} >> 1 \qquad (2)$$

The transformation (2) can be adapted to the "two-layer" MPI-OpenMP scheme, where a separate MPI-MAP executing process performs the transformation of

$$\{(\boldsymbol{\mu}_j, \boldsymbol{\mu}_{t_j}), j = \overline{1,m}\} \to \{(v_{1_j}, v_{2_j})^T, j = \overline{1,m}\} \qquad (3)$$

by parallelizing calculation of the values on the right side (3) based on OpenMP.

Numerical integration of the initial boundary value problem (1) is implemented by the Galerkin's projection method [4] and subsequent application of the BDF method to the resulting Cauchy problem for the system of ordinary differential equations.

5. Model of stabilization system

The object moves with respect to a fixed coordinate system $O_0 x_0 y_0 z_0$ (see fig. 2) under the action of force $\mathbf{P}$, attraction to the Earth and external disturbing horizontal force $\mathbf{F}_e = (0, F_{e_{y0}}, F_{e_{z0}})^T$.

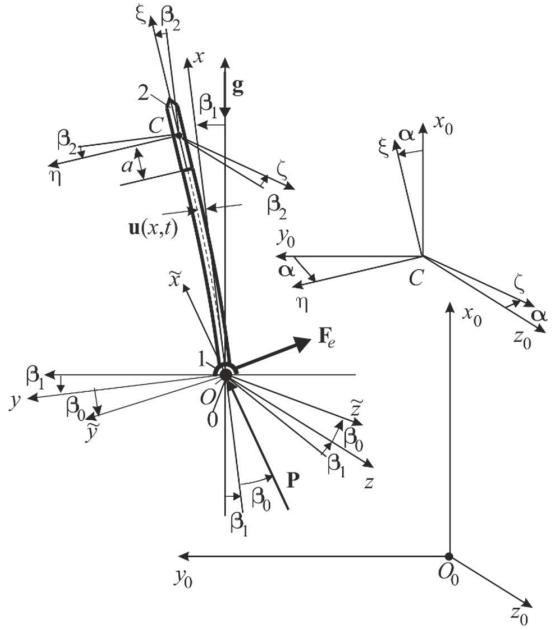

Fig. 2. Structural scheme

The coordinate system $Oxyz$ is connected to the body 1, and $\mathbf{r}_1 = (x_1, y_1, z_1)^T$ and $\boldsymbol{\beta}_1 = (\beta_{1,1}, \beta_{1,2}, \beta_{1,3})^T$ characterize its linear and angular displacements relative to $O_0 x_0 y_0 z_0$. Linear $\mathbf{r}_2 = (x_2, y_2, z_2)^T$ and angular $\boldsymbol{\beta}_2 = (\beta_{2,1}, \beta_{2,2}, \beta_{2,3})^T$ displacement of body 2 with respect to $Oxyz$ is caused by the elastic displacement $\mathbf{u} = (u_x, u_y, u_z)^T = \mathbf{u}(x, t)$ of the centerline of the hull. The rotation angle $\boldsymbol{\alpha} = (\alpha_1, \alpha_2, \alpha_3)^T$ of the body 2 relative to $O_0 x_0 y_0 z_0$ measures the gyrostabilizer, and the control moments of the forces $M_j^{(c)}$, $j = 1,2,3$ are formed. Under the action of $M_2^{(c)}$ and $M_3^{(c)}$ body 0 rotates at angles $\boldsymbol{\beta}_0 = (0, \beta_{0,2}, \beta_{0,3})^T$ relative to $Oxyz$. The moment $M_1^{(c)}$ acts on the body 1 and compensates for the rotation of the movable object relative to the longitudinal axis. Let $\boldsymbol{\omega}_0 = (\omega_{0_x}, \omega_{0_y}, \omega_{0_z})^T$, $\boldsymbol{\Omega}_1 = (\Omega_{1_x}, \Omega_{1_y}, \Omega_{1_z})^T$, $\boldsymbol{\Omega}_2 = (\Omega_{2_\xi}, \Omega_{2_\eta}, \Omega_{2_\zeta})^T$ be the relative and absolute angular velocities of bodies 0, 1, 2; $\mathbf{Q} = (Q_1, Q_2, Q_3)^T$, $\mathbf{M} = (M_1, M_2, M_3)^T$ be the internal forces and moments acting in the cross sections of the body. Here $\mathbf{x}(t) = (F_{e_{y0}}(t), F_{e_{z0}}(t))^T$ and $\mathbf{y}(t) = (\beta_{1,3}(t), \beta_{2,3}(t), \beta_{1,2}(t), \beta_{2,2}(t), \beta_{1,1}(t), \beta_{2,1}(t))^T$ are input and output vector functions, $\mathbf{p} = (p_1, p_2, \ldots, p_{12})^T$ are feedback parameters. The model equations of the nonlinear stabilization system are given in Appendix A. The set of parameters $\boldsymbol{\mu} = (\mu_1, \mu_2, \mu_3)^T$ characterizes typical nonlinearities, and the parameter $\boldsymbol{\mu}_t = \{\mu_4\}$, $\mu_4 \ge 0$ characterizes a smooth change in the characteristic overload according to the law

$$a_x(t) = a_x^{(\min)} + (a_x^{(\max)} - a_x^{(\min)}) e^{-\mu_4 t}, t \ge 0, a_x^{(\min)} < a_x \le a_x^{(\max)} \qquad (4)$$

At $\boldsymbol{\mu} = 0$, the model equations are linearized and decomposed into three independent subsets corresponding to the motion in the $O_0 x_0 y_0$ and $O_0 x_0 z_0$ planes (by virtue of symmetry, they pass into each other), as well as to the rotation relative to the longitudinal axis. In this case, $p_{5+j} = p_j$, $j = \overline{1,5}$, correspond to the stabilization system in the vertical direction, and p_{11}, p_{12} correspond to the stabilization system with respect to the longitudinal axis.

6. Numerical simulation results

In the numerical simulation of the output vector functions of the nonlinear angular stabilization system, the components of the input vector function were given as $F_{e_{y0}}(t) = 1(t), F_{e_{z0}}(t) = 1(t) - 1(t-1)$, where $1(t)$ is the unit jump function of Heaviside. For stabilization system with a set of parameters

$$J_0 = 0.02, m_1 = 0.3, J_1 = 0.07, m_2 = 0.2, J_2 = 0.05, a = 0.166667, a_x^{(\min)} = 0.2, a_x^{(\max)} = 2,$$
$$\gamma = 0.01, J_{1k} = 0.1, J_{2k} = 0.05, J_k = 2, \mu_1 = 0.08, \mu_2 = 0.15, \mu_3 = 0.055, \mu_4 = 0.05 \quad (5)$$

The feedback parameters of the stabilization system in the direction of vertical $p_1 = p_6 = 6.347$, $p_2 = p_7 = 13.12, p_3 = p_8 = 17.59, p_4 = p_9 = 14.03, p_5 = p_{10} = 5.951$ were chosen on the basis of an adaptive algorithm of parametric synthesis of the family of linearized models of HDS [4]. Since the stabilization of the object with respect to the longitudinal axis is intended to compensate for the slow accumulation of errors due to nonlinear effects, the feedback parameters $p_{11} = 0.04$, $p_{12} = 1$ are selected in the central part of the stability region.

Fig. 3 presents the results of numerical simulation of the components $\beta_{1,2}$ and $\beta_{1,3}$ of the output vector functions of the original nonlinear unsteady HDS (shown as a solid line) and its linear stationary analog at $\mu_1 = \mu_2 = \mu_3 = \mu_4 = 0$ (shown as a dashed line). The significant difference of the results is explained by the fact that the dimensionless overload a_x decreases smoothly, with the decrease of a_x in the considered range of overload changes in the linear stationary system, the attenuation of transients decreases, and the characteristic value of the output vector function increases. Nevertheless, parametric synthesis by the linearized model allows to stabilize the original nonlinear system in the vertical direction in the entire range of overloads. As follows from the results presented in Fig. 4, the selected values of the feedback parameters p_{11} and p_{12} allow to stabilize the movable control object with respect to the longitudinal axis, i.e. to compensate for the slow accumulation of errors due to nonlinear effects.

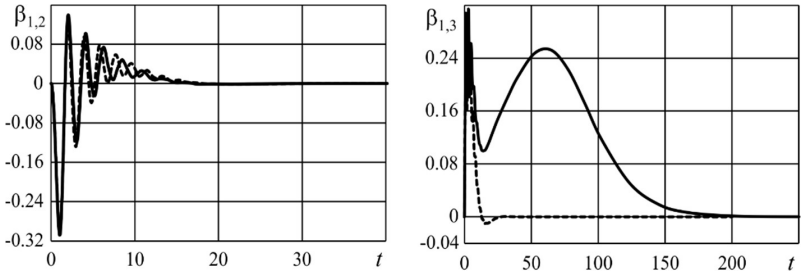

Fig. 3. Stabilization in the vertical direction

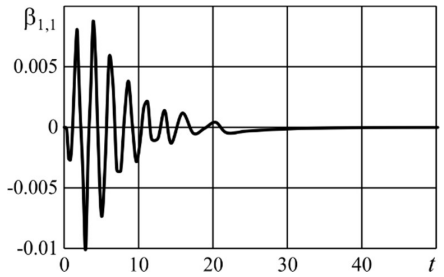

Fig. 4. Stabilization with respect to the longitudinal axis

Fig. 5 shows the dependences of the parameters $\mu_3 \in [0,0.055]$ and $\mu_4 \in [0,0.05]$ at fixed μ_1 and μ_2 maximum v_1 and standard v_2 deviations (see eq. (2)) of the output vector function of the nonlinear HDS on the output vector function of the linearized HDS for $t_{\max} = 250$. As follows from the data presented in Fig. 5, when changing the overload according to (9) the greatest influence on the output vector function of the nonlinear HDS has parameter μ_4, characterizing the unsteadiness of the system.

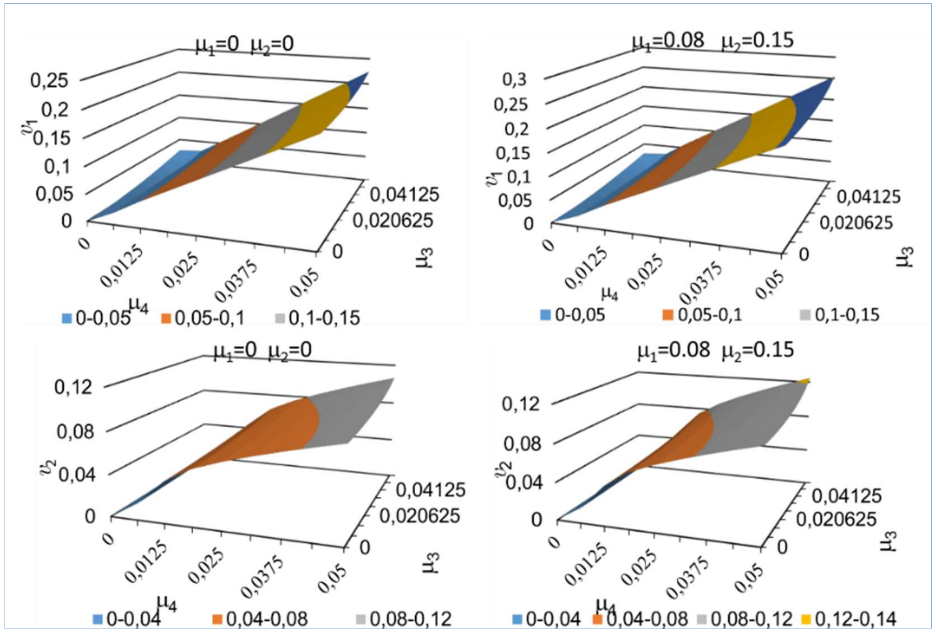

Fig. 5. Maximum and standard deviations

Similar data characterizing the efficiency of stabilization with respect to the vertical, longitudinal axis, as well as the influence of the parameters of nonlinearity and unsteadiness on the output functions of the stabilization system with parameters

$$J_0 = 0.00003, m_1 = 0.0667, J_1 = 0.00009728, m_2 = 0.333, J_2 = 0.00345, a = 0.166667, a_x = 1, \gamma = 0.01, p_1 = p_6 = 4.098, p_2 = p_7 = 9.553, p_3 = p_8 = 7.687, p_4 = p_9 = 7.714, p_5 = p_{10} = 3.269, J_{1k} = 0.002, J_{2k} = 0.005, J_2 = 2, \mu_1 = 0.08, \mu_2 = 0.2, \mu_3 = 0.04, \mu_4 = 0.05, p_{11} = 0.05, p_{12} = 1 \quad (6)$$

are shown in fig. 6-8. Similarly to the previously discussed non-linear stabilization system allows to compensate for the unwanted errors throughout the range of overload (see fig. 5, 6). The greatest influence on the output vector function of the nonlinear HDS has the parameter μ_4, which characterizes the unsteadiness of the system (see fig. 8).

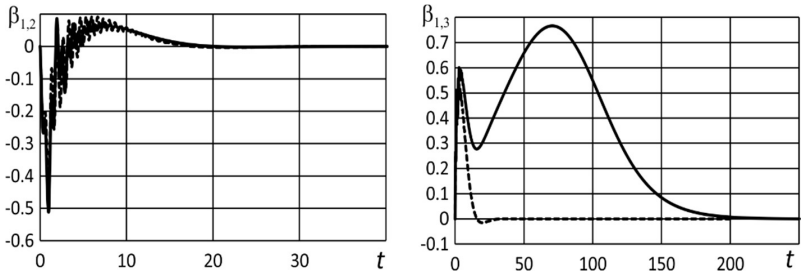

Fig. 6. Stabilization in the vertical direction

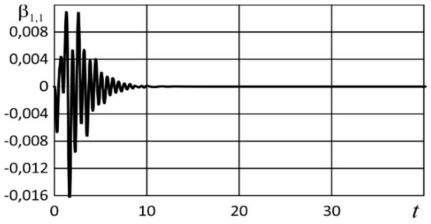

Fig. 7. Stabilization with respect to the longitudinal axis

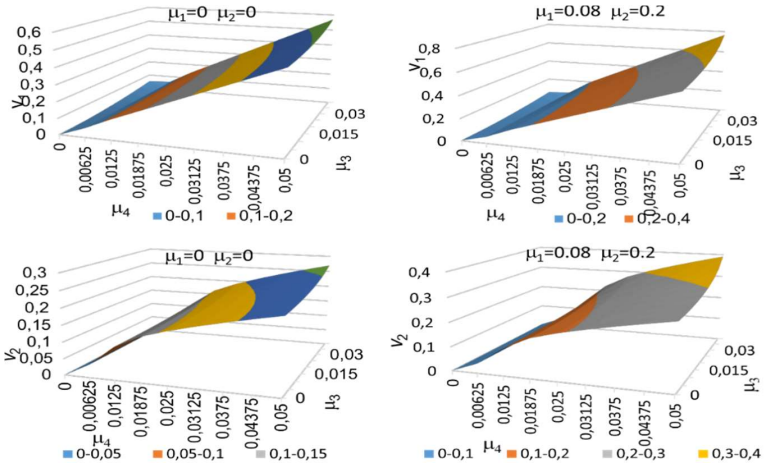

Fig. 8. Maximum and standard deviations

7. Efficiency analysis of parallel algorithms

Consider the effectiveness of the implementation on computer systems with coprocessors Intel Xeon Phi parallel algorithm (2), (3) modeling the effect of typical nonlinearities and unsteadiness on the output functions of the HDS. The data corresponding to the modeling of a nonlinear stabilization system with parameters (5) are presented in Table 1. The calculations were performed on a cluster of faculty of Computer Science and Informational Technologies and Volga Region Center of New Information Technologies of SSU. The four-dimensional grid of change of parameters $\mu_1, \mu_2, \mu_3\ \mu_4$ dimension $6 \times 9 \times 9 \times 9$ was used.

Table 1. Modeling of the impact of model nonlinearities and non-stationary, sec.

Grid 6 × 9 × 9 × 9					
Processor, serial/parallel	Test 1	Test 2	Test 3	Test 4	Test 5
Intel Xeon E5-2603 v2, serial	16411	16325	16470	16531	16314
2 processors Intel Xeon E5-2603 v2, OpenMP.	2480	2471	2501	2492	2485
Coprocessor Intel Xeon Phi 5110P, OpenMP	1667	1635	1673	1649	1655
2 coprocessors Intel Xeon Phi 5110P, MPI-MAP/OpenMP	1023	1015	1032	1008	1040

As follows from the Table 1 results, in this case, the use of a single Intel Xeon Phi coprocessor is more efficient than the use of two quad-core CPUs. The most profitable strategy of using coprocessors is parallelization based on OpenMP inside the coprocessor and parallelization based on MPI-MAP between coprocessors. Similar data for the stabilization system with parameters for the stabilization system with a set of parameters (6) are presented in Table 2. And in this case, using one Intel Xeon Phi processor is more efficient than using two quad-core CPUs. The most profitable strategy for the use of coprocessors is the parallelization based on OpenMP within the coprocessor and parallelization based on MPI-MAP between the coprocessors.

Table 2. Modeling of the impact of model nonlinearities and non-stationary, sec.

Grid 6 × 9 × 9 × 9					
Processor, serial/parallel.	Test 1	Test 2	Test 3	Test 4	Test 5
Intel Xeon E5-2603 v2, serial.	9637	9597	9645	9657	9675
2 processors Intel Xeon E5-2603 v2, OpenMP	1443	1470	1430	1412	1467
Coprocessor Intel Xeon Phi 5110P, OpenMP	1052	1042	1063	1037	1055
2 coprocessors Intel Xeon Phi 5110P, MPI-MAP/OpenMP	703	699	710	707	705

Analogical evidence of the effectiveness of the implementation of the parallel algorithm (2), (3) using a single Intel Xeon Phi coprocessor (OpenMP) and two Intel Xeon Phi coprocessors (MPI-MAP – OpenMP) for a more detailed meshes, changing parameters $\mu_1, \mu_2, \mu_3\ \mu_4$ are given in Table 3 for stabilization system with parameters (5) and in Table 4 for the stabilization system with parameters (6).

Table 3 - Modeling of the impact of model nonlinearities and non-stationary, sec.

Processor, serial/parallel.	Test 1	Test 2	Test 3	Test 4	Test 5
Grid 6 × 16 × 16 × 16					
Coprocessor Intel Xeon Phi 5110P, OpenMP	8953	9005	8934	8902	8985
2 coprocessors Intel Xeon Phi 5110P, MPI-MAP/ OpenMP	4726	4753	4715	4703	4744
Grid 12 × 16 × 16 × 16					
Coprocessor Intel Xeon Phi 5110P, OpenMP	18132	18243	18025	18187	18053
2 coprocessors Intel Xeon Phi 5110P, MPI-MAP/ OpenMP	9478	9529	9435	9501	9439

Table 4 - Modeling of the impact of model nonlinearities and non-stationary, sec.

Processor, technology of parallelization	Test 1	Test 2	Test 3	Test 4	Test 5
Grid 6 × 16 × 16 × 16					
Coprocessor Intel Xeon Phi 5110P, OpenMP	5671	5634	5654	5754	5698
2 coprocessors Intel Xeon Phi 5110P, MPI-MAP/ OpenMP	2988	2969	2967	3031	3002
Grid 12 × 16 × 16 × 16					
Coprocessor Intel Xeon Phi 5110P, OpenMP	11205	11278	11154	11174	11237
2 coprocessors Intel Xeon Phi 5110P, MPI-MAP/ OpenMP	5777	5809	5735	5741	5798

As follows from the Table 3 and 4 results, with an increase in the average number of nodes on the grid measurement, the multiplicative contribution to the acceleration of the MPI-MAP pattern quickly tends to the number of coprocessors used.

8. Conclusions

The proposed parallel algorithm is effective on cluster systems with nodes using processors with a large number of cores. In particular, it is effective on cluster systems with Intel Xeon Phi coprocessors.

References

[1] Andreichenko D.K., Andreichenko K.P. On the theory of hybrid dynamical systems. Journal of Computer and Systems Sciences International, vol. 39, no. 3, 2000, pp. 383-398.

[2] Andreichenko D.K., Andreichenko K.P. Modeling, analysis and synthesis of combined dynamical systems. Tutorial. Saratov, Rait-Ekspo Publ., 2013. 144 p. (in Russian) / Д.К. Андрейченко, К.П. Андрейченко. Моделирование, анализ и синтез комбинированных динамических систем. Учебное пособие. Саратов, Издательский дом «Райт-Экспо», 2013 г., 144 с.

[3] Andreichenko D.K., Andreichenko K.P., Melnichuk D.V. Pattern MPI-MAP and modeling of nonlinear hybrid dynamical systems. In Proc. of the IV International scientific conference on Problems of control, information processing and transmission, vol. 2, 2015, pp. 19-26 (in Russian) / Д.К. Андрейченко, К.П. Андрейченко, Д.В. Мельничук. Паттерн MPI-MAP и моделирование нелинейных комбинированных динамических систем. В сборнике трудов IV международной научной конференции «Проблемы управления, обработки и передачи информации», т. 2, 2015 г., pp. 19-26

[4] Andreichenko D.K., Andreichenko K.P., Melnichuk D.V., Portenko M.S. Adaptive Algorithm of Parametric Synthesis of Hybrid Dynamical Systems. Izvestiya of Saratov University. New Series. Series: Mathematics. Mechanics. Informatics, vol. 16, issue. 4, 2016, pp. 465–475 (in Russian) / Д.К. Андрейченко, К.П. Андрейченко, Д.В. Мельничук, М.С. Портенко. Адаптивный алгоритм параметрического синтеза комбинированных динамических систем. Известия Саратовского университета, новая серия, серия: Математика. Механика. Информатика, том 16, вып. 4, 2016 г., стр. 465-475.

[5] Kang Q., Träff J.L., Al-Bahrani R., Agraval A., Choundary A., Liao W. Scalable Algorithms for MPI Intergroup Allgather and Allgatherv. Parallel Computing, vol. 85, 2019, pp. 220-230.

[6] Dalcin L., Mortensen M., Keyes D.E. Fast parallel multidimensional FFT using advanced MPI. Journal of Parallel and Distributed Computing, vol. 128, 2019, pp. 137–150

[7] Avdeeva A.N., Puzikova V.V. Application of parallel algorithms for numerical simulation of quasi-one dimensional blood flow. Trudy ISP RAN/Proc. ISP RAS, vol. 30, issue 2, 2018, pp. 301-316 (in Russian) DOI: 10.15514/ISPRAS-2018-30(2)-15 / Авдеева А.Н., Пузикова В.В. Применение параллельных алгоритмов при численном моделировании кровотока в квазиодномерном приближении. Труды ИСП РАН, том 30, вып. 2, 2018 г., стр. 301-316.

[8] Towara M., Schanen M., Naumann U. MPI-Parallel Discrete Adjoint OpenFOAM. Procedia Computer Science, vol. 51, 2015, pp. 19-28.

[9] Tamada Y. Memory efficient parallel algorithm for optimal DAG structure search using direct communication. Journal of Parallel and Distributed Computing, vol. 119, 2018, pp. 27–35.

[10] Chen C., Pouransari H., Rajamanickam S., Boman E.G., Darve E. A distributed-memory hierarchical solver for general sparse linear systems. Parallel Computing, vol. 74, 2018, pp. 49–64.

[11] Takahashi D. Computation of the 100 quadrillionth hexadecimal digit of π on a cluster of Intel Xeon Phi processors. Parallel Computing, vol. 75, 2018, pp. 1–10.

[12] Cheng X., He B., Lu M., Lau C.T. Many-core needs fine-grained scheduling: A case study of query processing on Intel Xeon Phi processors. Journal of Parallel and Distributed Computing, vol. 120, 2018, pp. 395–404.

[13] Lazarev D.O., Kuzyurin N.N. On-line algorithm for scheduling parallel tasks on related computational clusters with processors of different capacities and its average-case analysis. Trudy ISP RAN/Proc. ISP RAS, vol. 30, issue 6, 2018, pp. 105-122 (in Russian). DOI: 10.15514/ISPRAS-2018-30(6)-6 / Лазарев Д.О., Кузюрин Н.Н. Алгоритм построения расписаний выполнения параллельных задач на группах кластеров с процессорам различной производительности и его анализ в среднем. Труды ИСП РАН, том 30, вып. 6, 2018 г., стр.105-122.

[14] Gandhi P. S., Borja P., Ortega R. Energy shaping control of an inverted flexible pendulum fixed to a cart. Control Engineering Practice, vol. 56, 2016, pp. 27–36.

Appendix A.

The rotation of the coordinate system is characterized by angles $\boldsymbol{\alpha} = (\alpha_1, \alpha_2, \alpha_3)^T$(in order $\alpha_3, \alpha_2, \alpha_1$), and

$$A(\boldsymbol{\alpha}) = \begin{bmatrix} \cos\alpha_3 & -\sin\alpha_3 & 0 \\ \sin\alpha_3 & \cos\alpha_3 & 0 \\ 0 & 0 & 1 \end{bmatrix} \begin{bmatrix} \cos\alpha_2 & 0 & \sin\alpha_2 \\ 0 & 1 & 0 \\ -\sin\alpha_2 & 0 & \cos\alpha_2 \end{bmatrix} \begin{bmatrix} 1 & 0 & 0 \\ 0 & \cos\alpha_1 & -\sin\alpha_1 \\ 0 & \sin\alpha_1 & \cos\alpha_1 \end{bmatrix}$$

$$B(\boldsymbol{\alpha}) = \begin{bmatrix} 1 & 0 & -\sin\alpha_2 \\ 0 & \cos\alpha_1 & \cos\alpha_2\sin\alpha_1 \\ 0 & -\sin\alpha_1 & \cos\alpha_2\cos\alpha_1 \end{bmatrix}$$

In dimensionless variables and parameters the equations of motion of the HDS have the form

$$\boldsymbol{\Omega}_1 = B(\mu_1\boldsymbol{\beta}_1)\dot{\boldsymbol{\beta}}_1, \boldsymbol{\Omega}_2 = A^T(\mu_1\beta_2)\boldsymbol{\Omega}_1 + B(\mu_1\boldsymbol{\beta}_2)\dot{\boldsymbol{\beta}}_2, \omega_{0_x} = -\dot{\beta}_{0,2}\sin(\mu_1\beta_{0,3})$$

$$\omega_{0_y} = \dot{\beta}_{0,2}\cos(\mu_1\beta_{0,3}), \omega_{0_z} = \dot{\beta}_{0,3}, m_1\ddot{\mathbf{r}}_1 = A(\mu_1\boldsymbol{\beta}_1)\mathbf{Q}(0,t) - \mathbf{F}_e +$$

$$+a_x[(1+m_2)A(\mu_1\boldsymbol{\beta}_1)\boldsymbol{\Phi}(0,\boldsymbol{\beta}_0) + m_1\boldsymbol{\Phi}(\boldsymbol{\beta}_1,\boldsymbol{\beta}_0)]$$

$$\boldsymbol{\Phi}(\boldsymbol{\alpha},\boldsymbol{\beta}) = \mu_1^{-1}(A(\mu_1\boldsymbol{\alpha})A(\mu_1\boldsymbol{\beta}) - E)(1,0,0)^T =$$

$$= (\Phi_1(\boldsymbol{\alpha},\boldsymbol{\beta}), \Phi_2(\boldsymbol{\alpha},\boldsymbol{\beta}), \Phi_3(\boldsymbol{\alpha},\boldsymbol{\beta}))^T, E = \mathrm{diag}\{1,1,1\}, J^{(1)} = \mathrm{diag}\{J_{1k}, J_1, J_1\}$$

$$J_0(\dot{\boldsymbol{\Omega}}_1 + \dot{\boldsymbol{\omega}}_0) + J^{(1)}\dot{\boldsymbol{\Omega}}_1 + \mu_1\boldsymbol{\Omega}_1 \times (J_0\boldsymbol{\omega}_0 + J^{(1)}\boldsymbol{\Omega}_1) = \mathbf{M}(0,t) - (M_c^{(1)}, 0, 0)^T$$

$$J_0\left[\dot{\Omega}_{1_y} + \dot{\omega}_{0_y} + \mu_1\left(\Omega_{1_z}\omega_{0_x} - \Omega_{1_x}\omega_{0_z}\right)\right] =$$

$$= M_2^{(c)}\cos\left(\mu_1\beta_{0,3}\right) + M_3^{(c)}\sin\left(\mu_1\beta_{0,3}\right)\sin\left(\mu_1\beta_{0,2}\right)$$

$$J_0\left[\dot{\Omega}_{1_z} + \dot{\omega}_{0_z} + \mu_1\left(\Omega_{1_x}\omega_{0_y} - \Omega_{1_y}\omega_{0_x}\right)\right] = M_3^{(c)}\cos\left(\mu_1\beta_{0,2}\right)$$

$$\alpha_2 = -\mu_1^{-1}\arcsin\left(\mu_1\Phi_3(\boldsymbol{\beta}_2,\boldsymbol{\beta}_1)\right), f_1(z) = \mathrm{tg}z \qquad (7)$$

$$\alpha_3 = \frac{1}{\mu_1}\arcsin\frac{\mu_1\Phi_2(\boldsymbol{\beta}_2,\boldsymbol{\beta}_1)}{\cos(\mu_1\alpha_2)}, \alpha_1 = -\frac{1}{\mu_1}\arcsin\frac{\mu_1\Phi_3^{**}(\boldsymbol{\beta}_2,\boldsymbol{\beta}_1)}{\cos(\mu_1\alpha_2)}$$

$$m_2\mathbf{w}_2 = a_x m_2[\boldsymbol{\Phi}(0,\mu_1(0,\beta_{2,2},\beta_{2,3})^T) - \boldsymbol{\Phi}^*(0,\mu_1\beta_1)] - A(\mu_1(0,\beta_{2,2},\beta_{2,3})^T)\mathbf{Q}(1,t)$$

$$\dot{\mathbf{w}}_2 = A^T(\mu_1\boldsymbol{\beta}_1)\ddot{\mathbf{r}}_1 + \dot{\boldsymbol{\Omega}}_1 \times \mathbf{R}_2 + \mu_1(\boldsymbol{\Omega}_1 \cdot \mathbf{R}_2)\boldsymbol{\Omega}_1 - \mu_1\boldsymbol{\Omega}_1^2\,\mathbf{R}_2 - 2\mu_1\boldsymbol{\Omega}_1 \times \dot{\mathbf{r}}_2 + \ddot{\mathbf{r}}_2$$

$$J^{(2)}\dot{\boldsymbol{\Omega}}_2 + \mu_1\boldsymbol{\Omega}_2 \times J^{(2)}\Omega_2 = -A^T((\mu_1\beta_{2,1},0,0)^T)\mathbf{M}(1,t) +$$

$$+(a,0,0)^T \times A^T((\mu_1\beta_{2,1},0,0)^T)\mathbf{Q}(1,t), J^{(2)} = \mathrm{diag}\{J_{2k}, J_2, J_2\}$$

$$\mathbf{R}_2 = (1+a,0,0)^T + \mu_1\mathbf{r}_2, \Phi^*(\boldsymbol{\alpha},\boldsymbol{\beta}) = \mu_1^{-1}(A^T(\mu_1\boldsymbol{\alpha})A^T(\mu_1\boldsymbol{\beta}) - E)(1,0,0)^T =$$

$$= (\Phi_1^*(\boldsymbol{\alpha},\boldsymbol{\beta}), \Phi_2^*(\boldsymbol{\alpha},\boldsymbol{\beta}), \Phi_3^*(\boldsymbol{\alpha},\boldsymbol{\beta}))^T$$

$$u'_x = \mu_1^{-1}[(1-\mu_1^2(u'^2_y + u'^2_z))^{1/2} - 1], L_{21} = \mu_1 u'_y, L_{31} = \mu_1 u'_z$$

$$L_{11} = (1 - L_{21}^2 - L_{31}^2)^{1/2}, L_{33} = (1 - L_{31}^2)^{1/2}, L_{12} = -L_{21}/L_{33}, L_{22} = L_{11}/L_{33}$$

$$L_{32} = 0, L_{13} = -L_{31}L_{22}, L_{23} = L_{31}L_{12}, \kappa_1 = u'_z(L_{12}L'_{22} - L_{22}L'_{12})$$

$$\kappa_2 = u'_z L_{22}L'_{11} - u''_y L_{23} - u''_z L_{33}, \kappa_3 = -\frac{u'_y L'_{11}}{L_{33}} + u''_y L_{22}$$

$$\ddot{u}_y + (A^T(\mu_1\boldsymbol{\beta}_1)\ddot{\mathbf{r}}_1)\cdot(0,1,0)^T - (\mu_1\dot{\Omega}_{1_x}u_z - \dot{\Omega}_{1_z}(x+\mu_1 u_x)) +$$

$$+\mu_1[(x+\mu_1 u_x)\Omega_{1_x} + \mu_1 u_z\Omega_{1_z}]\Omega_{1_y} - \mu_1^2(\Omega_{1_x}^2 + \Omega_{1_z}^2)u_y + 2\mu_1(\Omega_{1_x}\dot{u}_z -$$

$$-\Omega_{1_z}\dot{u}_x) = L_{21}(Q'_1 + \mu_1(\kappa_2 Q_3 - \kappa_3 Q_2)) + L_{22}(Q'_2 - \mu_1(\kappa_1 Q_3 - \kappa_3 Q_1)) +$$

$$+L_{23}(Q'_3 + \mu_1(\kappa_1 Q_2 - \kappa_2 Q_1)) - a_x[\Phi_2^*(0,\boldsymbol{\beta}_1) + ((m_2+1-x)u'_y)']$$

$$\ddot{u}_z + (A^T(\mu_1\boldsymbol{\beta}_1)\ddot{\mathbf{r}}_1)\cdot(0,0,1)^T + \mu_1\dot{\Omega}_{1_x}u_y - \dot{\Omega}_{1_y}(x+\mu_1 u_x) + \qquad (8)$$

$$+\mu_1[(x+\mu_1 u_x)\Omega_{1_x} + \mu_1 u_y\Omega_{1_y}]\Omega_{1_z} - \mu_1^2(\Omega_{1_x}^2 + \Omega_{1_y}^2)u_z - 2\mu_1(\Omega_{1_x}\dot{u}_y -$$

$$-\Omega_{1_y}\dot{u}_x) = L_{31}(Q'_1 + \mu_1(\kappa_2 Q_3 - \kappa_3 Q_2)) + L_{33}(Q'_3 + \mu_1(\kappa_1 Q_2 - \kappa_2 Q_1)) -$$

$$-a_x\left[\Phi_3^*(0,\boldsymbol{\beta}_1) + \left((m_2+1-x)u'_z\right)'\right]$$

$$Q''_1 - \mu_1^2(\kappa_2^2 + \kappa_3^2)Q_1 = \mu_1\{-a_x(m_2 + 1 - x)(\kappa_2^2 + \kappa_3^2) + \kappa'_3 Q_2 - \kappa'_2 Q_3 +$$
$$+2\kappa_3 Q'_2 - 2\kappa_2 Q'_3 - \mu_1\kappa_1(\kappa_2 Q_2 + \kappa_3 Q_3) - ((\dot{u}'_x)^2 + (\dot{u}'_y)^2 + (\dot{u}'_z)^2) +$$
$$+(\Omega_{1_x} L_{11} + \Omega_{1_y} L_{21} + \Omega_{1_z} L_{31})^2 - (\Omega_{1_x}^2 + \Omega_{1_y}^2 + \Omega_{1_z}^2) +$$
$$+2[L_{11}(\Omega_{1_y}\dot{u}'_z - \Omega_{1_z}\dot{u}'_y) - L_{21}(\Omega_{1_x}\dot{u}'_z - \Omega_{1_z}\dot{u}'_x) + L_{31}(\Omega_{1_x}\dot{u}'_y - \Omega_{1_y}\dot{u}'_x)]\}$$

$$u_y(0,t) = 0, u'_y(0,t) = 0, u_y(1,t) = y_2 - a\Phi_2(0,\boldsymbol{\beta}_2), u'_y(1,t) = \cos(\mu_1\beta_{2,2}) \cdot$$
$$\cdot \mu_1^{-1}\sin(\mu_1\beta_{2,3}), u_z(0,t) = 0, u'_z(0,t) = 0, u_z(1,t) = z_2 - a\Phi_3(0,\boldsymbol{\beta}_2),$$
$$u'_z(1,t) = -\mu_1^{-1}\sin(\mu_1\beta_{2,2}), x_2 = u_x(1,t) + a\Phi_1(0,\boldsymbol{\beta}_2),$$
$$Q'_1(0,t) + \mu_1\big(\kappa_2(0,t)Q_3(0,t) - \kappa_3(0,t)Q_2(0,t)\big) = \quad (9)$$
$$= \ddot{\mathbf{r}}_1 \cdot A(\mu_1\boldsymbol{\beta}_1)(1,0,0)^T + a_x\Phi_1^*(0,\boldsymbol{\beta}_1)$$
$$Q'_1(1,t) + \mu_1(\kappa_2(1,t)Q_3(1,t) - \kappa_3(1,t)Q_2(1,t)) =$$
$$= a_x\Phi_1^*(\boldsymbol{\beta}_2,\boldsymbol{\beta}_1) + \mu_1 a(\Omega_{2_\eta}^2 + \Omega_{2_\zeta}^2) + (1,0,0)^T \cdot A^T(\mu_1\boldsymbol{\beta}_2)\mathbf{w}_2$$

$$M_1 = I_k\left(\beta_{2,1} + \gamma\dot{\beta}_{2,1} - \int_0^1 \kappa_1 dx\right), M_2 = \kappa_2 - \gamma\dot{u}''_z, M_3 = \kappa_3 + \gamma\dot{u}''_y \quad (10)$$
$$Q_2 = -M'_3 + \mu_1(\kappa_2 M_1 - \kappa_1 M_2), Q_3 = M'_2 + \mu_1(\kappa_3 M_1 - \kappa_1 M_3)$$
$$\boldsymbol{\beta}_1(0) = \dot{\boldsymbol{\beta}}_1(0) = \boldsymbol{\beta}_2(0) = \dot{\boldsymbol{\beta}}_2(0) = \beta_{0,2}(0) = \dot{\beta}_{0,2}(0) = \beta_{0,3}(0) = \dot{\beta}_{0,3}(0) =$$
$$= \mathbf{r}_1(0) = \dot{\mathbf{r}}_1(0) = y_2(0) = \dot{y}_2(0) = z_2(0) = \dot{z}_2(0) = \quad (11)$$
$$= u_y(x,0) = \dot{u}_y(x,0) = u_z(x,0) = \dot{u}_z(x,0) = 0$$

Here (7) are ordinary differential equations, (8) are partial differential equations, (9) are boundary conditions, (10) are constraint's conditions, (11) are initial conditions, $()' = \partial()/\partial x$.

Информация об авторе / Information about author

Дмитрий Вадимович МЕЛЬНИЧУК получил степень магистра по направлению «Прикладная математика и информатика» в Саратовском национальном исследовательском государственном университете имени Н.Г. Чернышевского, Саратов, Россия. Его исследовательские интересы включают математическое моделирование, моделирование управляемых комбинированных динамических систем, параллельные алгоритмы и параллельные вычислительные технологии.

Dmitry Vadimovich MELNICHUK received a master's degree in «Applied mathematics and Informatics» at Saratov State University, Saratov, Russia. His research interests include mathematical modeling, simulation of controlled hybrid dynamic systems, parallel algorithms, and parallel computing.